ANALYSIS OF SHELL MODELS IN RELATION TO A NEW SELF-SIMILARITY THEORY OF THE INERTIAL RANGE

ANALYSIS OF SHELL MODELS IN RELATION TO A NEW

SELF-SIMILARITY THEORY OF THE INERTIAL RANGE

IN ISOTROPIC HOMOGENOUS TURBULENCE

A Dissertation Presented to the Graduate Faculty of the

Dedman College: School of Humanities and Sciences

Southern Methodist University

in

Partial Fulfillment of the Requirements

for the degree of

Doctor of Philosophy

with a

Major in Computational and Applied Mathematics

by

Jennifer A. Tarin

(B.S., Texas Woman's University, 2004)
(M.S., Southern Methodist University, 2006)

August 4, 2009

ACKNOWLEDGMENTS

Write who you'd like to thank here. I would like to thank the Department of Mathematics of Southern Methodist University.

Tarin , Jennifer A.

B.S., Texas Woman's University, 2004

M.S., Southern Methodist University, 2006

Analysis of Shell Models in Relation to a New

Self-Similarity Theory of the Inertial Range

in Isotropic Homogenous Turbulence

Advisor: Professor Mogens V. Melander

Doctor of Philosophy degree conferred August 4, 2009

Dissertation completed August 4, 2009

We investigate the question of similarity in homogenous isotropic turbulence using the well known shell models, GOY and Sabra. These **e**2.886171.482289(e)-4/W1/5(m)2.9243465

TABLE OF CONTENTS

LIST OF FIGURES

LIST OF TABLES

Write something here. I dedicate this thesis to someone important to me.

Chapter 1

INTRODUCTION

In this thesis we focus on the simplest possible turbulence in three dimensional incompressible fluid. The whole space is filled with fluid so there are no confining walls and corresponding boundary layers. Moveover, the turbulence is homogeneous, isotropic, and driven into statistical equilibrium by a strong steady large scale forcing. This results in a high Reynolds number. In principle, we are interested in the limit of infinite Reynolds number. This limit is particularly interesting because of the behavior of the dissipation - namely, there is nonzero dissipation in the limit of vanishing viscosity. Therefore, the Euler equations do not apply as they have no dissipation term. The dynamics and statistics at scales much smaller than the forcing scale are believed to be universal, e.g. [7]. That is, independent of the particulars of the forcing. For this reason, the small scales (small relative to the forcing scale) are commonly referred to as the universal equilibrium range. In turn, this range divides into two parts: the dissipation range and the inertial range (or subrange). In the inertial range, the scales are large enough for the dissipation to be negligible. In other words, inertial forces alone rule this area. Our interest is the statistics of turbulence in the inertial range. The classical view is that it should have universal properties.

There is much debate about what those universal properties might be. Some even argue against universality altogether. An old idea dating back to Kolmogorov 1941 [11] suggests scale invariance of the statistics in the inertial range. In other words, the inertial range might exhibit self-similarity. The governing equations - Navier Stokes equations in Fourier space - certainly suggest so because the viscous

1

term can be neglected in the inertial range and the rest can be expressed in scale independent form. The idea of universal self-similarity goes a significant step beyond just universality.

The first self-similarity that comes to mind was suggested by Kolmogorov and is known as statistical self-similarity. This particular self-similarity is contradicted by both experimental and computational evidence e.g. [7]. The subject of this thesis is to investigate another type of self-similarity proposed in [14, 15, 16].

1.1. Homogeneous Isotropic Turbulence

The governing equations are the incompressible Navier Stokes equations:

$$\frac{\partial \mathbf{u}}{\partial t} + (\mathbf{u} \cdot \nabla)\mathbf{u} = -\frac{1}{\rho}\nabla p + \nu \nabla^2 \mathbf{u} + \mathbf{F}, \tag{1.1}$$

$$\nabla \cdot \mathbf{u} = 0, \tag{1.2}$$

where $\mathbf{u}$ is the flow velocity, ρ is the fluid density, $\mathbf{p}$ is the pressure, ν is the kinematic viscosity, and $\mathbf{F}$ is the forcing. The density is constant so there are no buoyancy effects. The viscosity is also constant. Moreover, the fluid is unbounded so there are no walls and boundary layers. We consider an idealized forcing specified in wave number space at a single spatial frequency so that we have homogeneity and isotropy. Under these circumstances we can transform the entire problem to Fourier space. There, a single equation describes the problem:

$$\left(\frac{\partial}{\partial t} + \nu k^2\right)\hat{u}_i(\mathbf{k}, t) = -ik_n P_{ij}(\mathbf{k})\int_{p+q=k}\hat{u}_j(\mathbf{p}, t)\hat{u}_n(\mathbf{q}, t)d\mathbf{p} + \hat{F}_i(\mathbf{k}), \qquad i$$

is the projection operator that removes the pressure term. This is the traditional starting point for the study of homogeneous isotropic turbulence [3, 10, 13] which always develops when the forcing is strong enough to give a high Reynolds number.

Homogeneity and isotropy refers to independence of location and orientation in space. The first to utilize this type of turbulence was G.I. Taylor [23]. With these properties it makes sense to talk aboutrae tbe

in Figure 1.1. In particular, the inertial range obeys a power law with slope $-5/3$ or nearly so. The $-5/$

1.4. Methods for Obtaining Data from the Inertial Range

In order to study the inertial range, we need to obtain numeri

they do not admit for power law scaling in the inertial range. Chapter **??** investigates pdf's constructed from given scaling exponents. In particular, we look at the log Poisson model of anomalous scaling [21]. We find that the pdf has a number of strange and undesirable features. Chapter **??** presents an analytic example of a pdf that is self-similar yet satisfies the power law requirement with nonlinear exponents. This provides a specific example that anomalous scaling may be expressed through self-similarity; an idea that was believed to have sunk with K41. This is a specific example from the new theory proposed in [14]. Chapter **??** introduces the shell models which will be used to generate inertial range data for our analysis in subsequent chapters. Shell models are severe truncations of the Navier Stokes equations in Fourier space. We chose two specific models; GOY and Sabra, both are well known. Both shell models are crudely analogous to spectral Navier Stokes equa

Chapter 2

## 2.1. Determination of n_0 and C_3 via Rescaled Structure Functions

When we previously defined structure functions, we neglected to include an intrinsic length scale. The intrinsic scale plays an important role in regard to the scaling coefficients, $\tilde{\mathbf{C}}_p$. Without an intrinsic scale, the coefficients cannot be described in universal terms. The reason is that any factor of the form 2

The common point of intersection forms the virtual origin for the inertial range. That is, the scaling laws cannot be continued to larger scales (smaller $\mathbf{n}$). In fact, $\mathbf{n_0}$ is the smallest $\mathbf{n}$ for $\mathbf{S}_p(\mathbf{n})$ in (2.5) that corresponds to a pdf.

Figure 2.1 is significant for many reasons. Not only does it determine an intrinsic length scale for the inertial range, and confirm the theoretical coefficient formula (2.4), it also shows that all $\mathbf{S}_p(\mathbf{n})$ can be computed from $\mathbf{S}_p(\tilde{\mathbf{n}})$ and the virtual origin, where $\tilde{\mathbf{n}}$ represents a single shell l 838(˜)-2.26269]TJ/R2481.64014m9.5649399(r)-0.649399(i)0.972

n
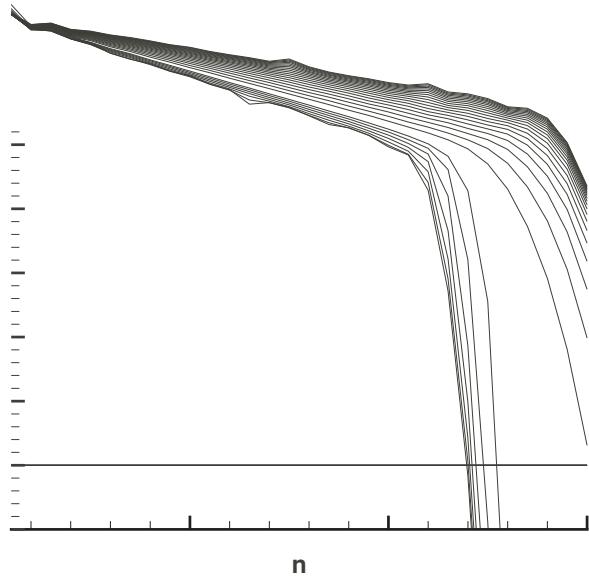
$$A = \frac{a-b}{c-d} \tag{2.15}$$

$$B = \frac{bc-ad}{b-a}. \tag{2.16}$$

Figure **??** shows the vertical and horizontal shifts as functions of n. We observe that both are linear functions of n as called for by the theory. The scatter around the regression line is in part due to the matching of the graphical objects being done manually. The theory does provide analytical formulas to do a computational collapse. However, the data we obtained contained too much statistical noise. Therefore, we were not able to use the analytical formulas. The vertical shift is also shown. It forms a straight line on log-log scales. Consequently, the stretching is a power law in $(n-n_0)$ just as predicted by the theory. The slope is $1/$ and we obtain $= 1.23$ from the regression line.

Table 2.1. Measurements for scaling individual radial profiles. Shell 12 is selected as the radial profile to be scaled to. The fixed scale refers to the Shell 12 axis. The first
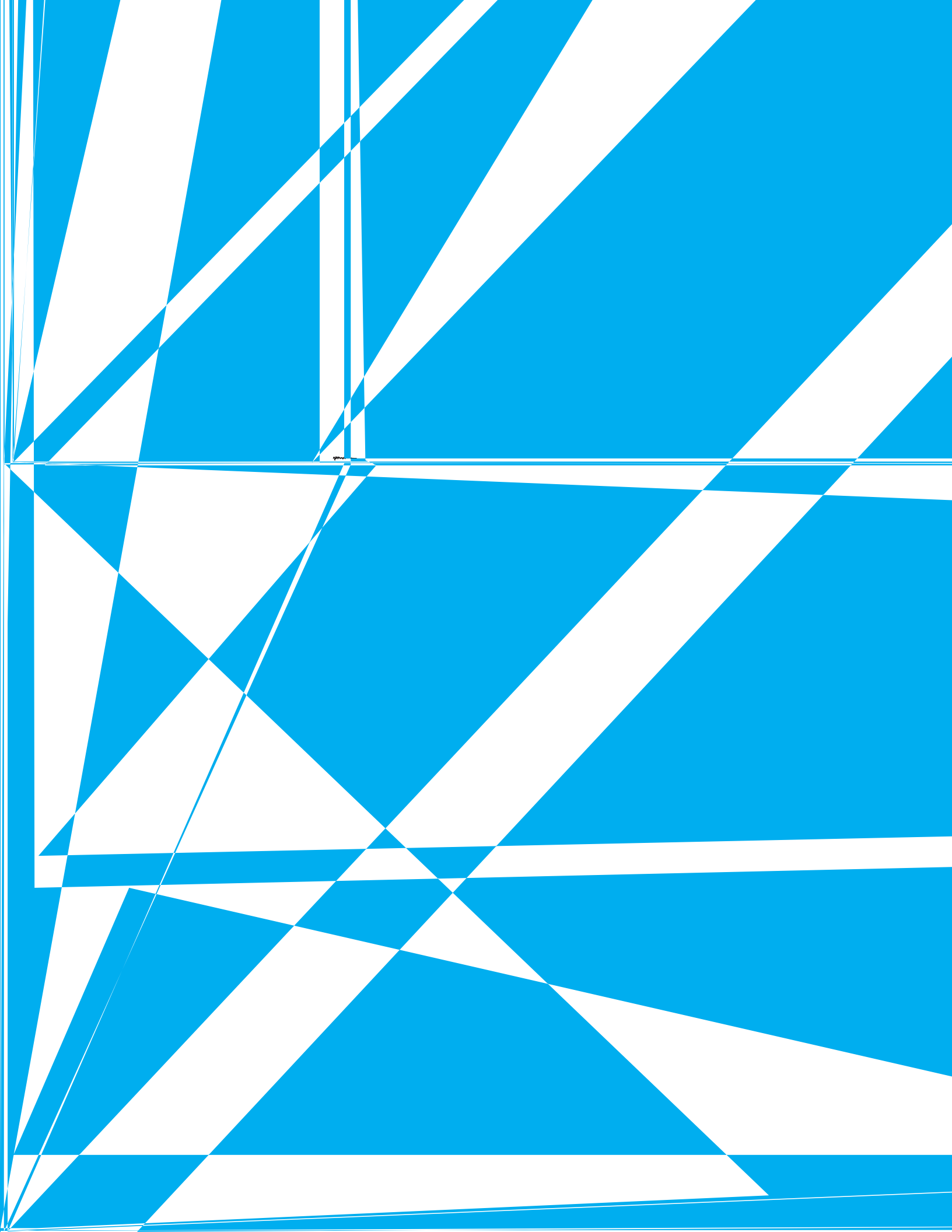
Appendix A

APPENDIX

A.1. Description of GOY Shell Model Runs and Table

In most cases, we have forced the models in the first shell so that the inertial range forms on the ultraviolet side. However, in run 2 from Table A.1, we force in shell seven and observe an infra-red inertial range form. Run 1 uses the parameters of [26] originally used. This run is used as a control and to reproduce Pisarenko et. al. [19] work. Run 2 is equivalent to Run 1 as far as the parameters are concerned. However, in this run, we force in shell 6. As a result, we see an infra-red inertial range. We can apply the affine collapse to this data as well. This result is of interest in the light of Carl Gibson idea that the true cascade in turbulence is from small to large scales [8]. We start with small forcing in Run 3. Here, the forcing is small enough that the solution is quasi-periodic and we have no inertial range. We can observe this in the distribution of $\mathbf{u}_n$. In this particular case, the points were located in a ring that was centered at the origin (see Figure A.1). However, there is still circular symmetry about the origin in this case.

In order to obtain an inertial range which the new similarity theory requires, we increase the forcing for Run 4. In Run 4, we still have virtually no inertial range. We must increase the forcing further. In Run 5, the model is chaotic and we have somewhat more of an inertial range. Run 6 increases the forcing and the shell number, however we are not obtaining enough of an inertial range. In Run 7, we increase the forcing significantly. The number of shells remains the same, but this time, we observe a distinct inertial range. We want to observe how much forcing we can pump into the

system before numerical problems arise. Thus, we create Run 8 and Run 9. Run 10 is

REFERENCES

[1] *On the singularity structure of fully developed turbulence* (Amsterdam, 1983), North-Holland.

[2] **Anselmet, F., Gagne, Y., Hopfinger, E. J., and Antonia, R. A.** High-order velocity structure functions in turbulent shear flows. *Journal of Fluid Mechanics 140*, -1 (1984), 63–89.

[3] **Batchelor, G.** *The theory of homogeneous turbulence.* Cambridge University Press, Cambridge, 1971.

[4] **Champagne, F. H.** The fine-scale structure of the turbulent velocity field. *Journal of Fluid Mechanics 86*, 01 (1978), 67–108.

[5] **Ditlevsen, P.** Cascades of energy and helicity in the goy shell model of turbulence. *Phys. Fluids 9*, 5 (1997), 1482–1484.

[6] **Ditlevsen, P., and Mogensen, I.** Cascades and statistical equilibrium in shell models of turbulence. *Phys. Rev. E 53*, 5 (1996), 4785–4793.

[7] **Frisch, U.** *Turbulence.* Cambridge University Press, Cambridge, 1999.

[8] **Gibson, C.** Turbulence in the ocean, atmosphere, galaxy, and universe. *Appl. Mech. Rev. 49*, 5 (1996), 299–315.

[9] **Grant, H. L., Stewart, R. W., and Moilliet, A.** Turbulence spectra from a tidal channel. *Journal of Fluid Mechanics Digital Archive 12*, 02 (1962), 241–268.

[10] **Hinze, J.** *Turbulence; an introduction to its mechanism and theory.* McGraw-Hill, New York, 1959.

[11] **Kolmogorov, A.** The local structure of turbulence in incompressible viscous fluid for very large reynolds numbers. *Reprinted Proc. R. Soc. Lond. (1991) 434*, 1890 (1941), 9–13.

[12] **Lundgren, T.** Inertial range scaling law. *Journal of Turbulence 6*, 22 (2005).

[13] **McComb, W.** *The Physics of Fluid Turbulence.* Clarendon Press, Oxford, 1991.

[14]